

Final Project Report for 08HQGR0041

**Analog and Numerical Simulation of Fault
Complexity of the San Gorgonio Knot**

Michele Cooke

Geosciences Department
University of Massachusetts, Amherst
611 North Pleasant St
Amherst, MA 01003-9297

cooke@geo.umass.edu

voice: 413-577-3142

FAX: 413-545-200

Term of award: 1/1/08-12/231/08

Project Report Submitted:

Abstract

Three-dimensional numerical and analog models are needed to investigate the role of non-vertical strike-slip fault segments on the deformation within restraining bends. Numerical models simulate geologic deformation of two alternative three-dimensional present-day configurations for the San Andreas Fault (SAF) through the restraining bend within the San Gorgonio Pass region (SGPR) in southern California. Both models produce decreasing strike-slip rates southward along the San Bernardino strand of the SAF similar to geologic data. The north-dipping SAF model better matches the available strike-slip data as well as the geologic uplift data for the southern San Bernardino Mountains than the vertical SAF model. We conclude that a north-dipping fault configuration is preferred for models of the SAF in the SGPR. The complexity of the active fault geometry at the SGPR promotes the transfer of strike-slip from the SAF, to the nearby but unconnected San Jacinto fault. Slip rates and uplift patterns are sensitive to fault geometry within strike-slip restraining bends.

Analog models are also used to explore the deformation field around the San Andreas fault. Results show that the clay models have greater off-fault strain and less fault slip than the elastic numerical models. The distribution of slip and the distribution of uplift matches geologic observations. This positive comparison supports the use of analog models to simulate deformation within southern California.

Introduction

Restraining bends along strike slip faults are traditionally believed to be composed of vertical strike-slip fault segments that curve along strike. However, two of the best-known restraining bends, the Santa Cruz and the San Bernardino Mountains (SBMs), California, may be associated with active non-vertical segments of the San Andreas fault (e.g. Allen, 1957, Anderson, 1990; Matti et al., 1992; Nicholson, 1996; Yule and Sieh, 2003; Carena et al., 2004). As geophysical studies reveal greater details of active strike-slip fault geometry within restraining bends, we require three-dimensional models that can fully investigate the contribution of non-vertical strike-slip faults to local deformation.

At the San Gorgonio Pass region (SGPR) of southern California the San Andreas fault (SAF) steps left in a restraining bend that has evolved into a complex network of active and formerly active, dipping and vertical, three-dimensionally irregular fault surfaces (Figure 1; e.g., Matti et al. 1985). Although field and geophysical investigations reveal active north-dipping thrust faults through the SGPR (e.g., Allen, 1957, Matti et al., 1992; Nicholson, 1996; Yule and Sieh, 2003; Carena et al., 2004; Langenheim et al., 2005), crustal deformation and earthquake rupture models simplify the SAF as vertical through this region (e.g., Meade and Hager, 2005; Olsen et al., 2006; Smith and Sandwell, 2006). Within these simplified fault models, slip vectors are primarily strike-slip and the models neglect the reverse slip documented on the north-dipping San Gorgonio Thrust (Yule and Sieh, 2003). As a consequence, physical aspects of earthquake rupture dynamics and the regional seismic hazard may go uncharacterized. Models of the southern SAF with geologically realistic geometry, which are now possible at relatively high resolutions, may lead to more accurate assessment of earthquake hazards for southern California. Such models are of timely importance as the segments of the southern San Andreas Fault (SAF) south of the Cajon Pass have not slipped substantially enough to release accumulated strain and may be nearing the end of their recurrence intervals (e.g., Yule et al., 2001; Weldon et al., 2004; Weldon et al., 2005).

We use the Boundary Element Method (BEM) to numerically simulate geologic timescale crustal deformation of two different SAF configurations, through the SGPR. The BEM modeling technique uses a triangular mesh to accurately replicate three-dimensionally irregular fault surfaces. Using this mesh, we have developed the first crustal deformation model of the southern SAF that incorporates geologically constrained north-dipping fault segments. We compare the model results to geologic observations and offer a preferred fault configuration for the SAF through the restraining bend of the SGPR. Our study reveals the sensitivity of slip distribution and uplift pattern to fault configuration through a restraining bend and may guide future models in other regions.

Geologic Uplift and Slip Rates

The SGPR contains a complex network of strike-slip and thrust faults. Between the vertical strike-slip segments of the SAF north and south of the San Geronio Pass (i.e., the San Bernardino strand and Coachella Valley segment of the SAF), Yule and Sieh (2003) documented two active north dipping fault strands of the San Andreas, the San Geronio thrust (SGT) and the Garnet Hill fault (Figure 1). Microseismicity in the region suggests that these faults maintain their north dip of 45–85° at depth (Carena et al., 2004). Both the observed and interpreted north dip on these two faults refute the presence of a vertical through-going strand of the SAF within the SGPR (Figure 2; Yule and Sieh, 2003; Carena et al., 2004).

Low-temperature thermochronometry at the Yucaipa Ridge, located between the now inactive Mill Creek strand and the active San Bernardino strand of the SAF, indicates ~3–6 km of uplift in the last 1.8 My (Spotila et al., 2001). While the time averaged uplift rate of the Yucaipa Ridge is 1.7 – 3.3 mm/yr, uplift was faster ca. 1.5 Ma than in the recent past (Spotila, et al., 2001). Offset markers across the SGT show 1 mm/yr relative uplift over the past 13 Ky (Yule and Sieh, 2003). Spatial variations in uplift rates are expected due to local fault geometry.

Geologic studies have revealed variable strike-slip rates along both the SAF and San Jacinto fault (SJF) within the SGPR. Near the Cajon Pass, Weldon and Sieh (1985) found 24.5 ± 3.5 mm/yr strike-slip along the SAF Southward, rates decrease along the San Bernardino strand to 11 – 16 mm/yr at Badger Canyon (McGill et al., 2007) to 3 – 17 mm/yr at Plunge Creek (McGill et al., 2006), and to 2.6 – 7.0 mm/yr at Burro Flats (Orozco, 2004). Where the San Bernardino strand intersects the SGT and Garnet Hill strand of the SAF the strike-slip rate decreases to 5.7 ± 0.8 mm/yr (Yule and Sieh, 1997). The northern Coachella Valley segment of the SAF slips 9 – 15 mm/yr (Behr et al., 2007). Along the SJF, strike-slip rates vary from >20 mm/yr at site 7 (Figure 1; Kendrick et al., 2002) to >9.2 mm/yr from alluvial fan offsets (Rockwell et al., 1990). In addition to strike-slip rates in the region, Yule and Sieh (2003) found a minimum of 2.5 mm/yr reverse-slip on the SGT.

San Andreas Model Alternatives

Two different fault geometries for active faults in the SGPR were created based on the Southern California Earthquake Center Community Fault Model (CFM), a compilation of active faults in southern California (Plesch et al., 2007). The first model has a simplified vertical fault geometry for the SAF within the SGPR. The second model follows the preferred configuration of the CFM (Carena et al., 2004; Plesch et al., 2007) and includes a 45–85° north-dipping Garnet Hill strand and SGT (Figure 2B). In both models, the faults are freely-slipping to a depth of 35 km where they intersect a horizontal freely-slipping crack that decouples crustal deformation from the modeled half space (Figure 3). The 35 km depth is chosen to match the imaged depth of the

Mohorovi_i discontinuity in this region (Magistrale et al., 2000). Within the model, discrete fault surfaces below the seismogenic crust simulate distributed deformation expected at these depths. Rather than prescribing slip along the faults within the SGPR, the weak faults of our model slip and interact in response to regional plate motions of 45 mm/yr N52°W right-lateral displacement (e.g. Bennett et al, 1999; Shen et al., 2003) applied at the edges of the horizontal crack.

Model Configuration

The models include the Mojave segment and the Coachella Valley segment of the San Andreas fault, as well as the San Jacinto Valley strand and the Anza segment of the San Jacinto fault. The San Gorgonio Pass region is comprised a complex array of formerly and presently active faults. For this model we focused on faults that exhibit significant recent activity. For example, the western portion of the mapped San Gorgonio thrust was not included in the model due to lack of recent activity. The San Bernardino strand of the San Andreas fault was included in the model because paleoseismicity shows this fault to be one of the major strands through the pass (Weldon and Sieh, 1985; McGill et al., 2007; McGill et al., 2002; Orozco, 2004). Subtle pressure ridges and hanging walls near the southern most surface trace of the San Bernardino strand suggest that the fault merges with the eastern portion of the San Gorgonio thrust (Yule and Sieh, 2003). Within the model, the San Gorgonio thrust has a north dip of 45-70°, and merges to the east with the Garnet Hill strand of the San Andreas Fault. The Garnet Hill strand dips to the north at 55-85°, and parallels the Banning strand. Both the Garnet hill and the Banning faults are believed to be active north of Palm Springs. For simplicity, we only include the Garnet Hill strand to represent deformation on both of these active parallel fault strands. Seismicity indicates that the Garnet Hill strand of the San Andreas fault extends from the San Gorgonio thrust to the Coachella Valley segment of the San Andreas fault even though geologic mapping does not show a surface trace intersection between the two faults (Langenheim et al., 2005). All of the three-dimensional faults included in the models have been smoothed at depth to remove any small irregularities observed along the fault trace at the Earth's surface that are unlikely to extend to significant depths.

Though the San Jacinto is made up of many en echelon faults (Sharp 1975), our models consider the fault to be continuous and connected. Delineating the San Jacinto fault into individual echelon strands may decrease the strike-slip rates on the San Jacinto fault but is not expected to substantially change the slip rates along the San Andreas fault strands within the San Gorgonio Pass region.

Poly3D Modeling Method

The models are run using Poly3D, a three dimensional Boundary Element Method (BEM) modeling code (Thomas, 1993). For this study, the BEM code is used to simulate the three-dimensional active faulting near the San Gorgonio Pass inside a linear elastic half-space. The triangular elements used in Poly3D are ideal for complex geometries characteristic of the active faults in the San Gorgonio Pass region. Fine meshes of triangular Poly3D elements have previously been used to simulate geologic deformation in the Los Angeles Basin (Griffith and Cooke, 2004; Griffith and Cooke, 2005; Cooke and Marshall, 2006; Meigs et al, 2008) and in the Ventura Basin (Marshall et al., in press). Within our models, the average diameter of elements along the San Andreas and San Jacinto faults is ~5 km and the element diameter decreases to

~2.5 km along the complex fault segments within the San Gorgonio Pass. The detail of this mesh permits accurate simulation of fault irregularities larger than 10 km.

Modeled Vertical Deformation Patterns

The surface uplift maps reveal significant differences between the vertical and north-dipping SAF models (Figure 4). The vertical configuration produces far less relative surface uplift than the north-dipping configuration. The greater uplift rates on the hanging wall of the north dipping SAF model are due to significant reverse slip rates on the dipping fault segments. The average reverse slip rate on the modeled SGT, 3.6 mm/yr, matches geologic observations (>2.5 mm/yr; Yule and Sieh, 2003). The north-dipping model has the greatest relative uplift in the areas of the Yucaipa Ridge block and the Morongo block (Figure 1), which have been uplifted at higher rates than the surrounding area (Spotila et al., 2001). The relative uplift rates produced by the north-dipping fault model at the Yucaipa Ridge (~1.6–1.9 mm/yr) fall within the lower half of time averaged geologic uplift rates, (1.6–3.3 mm/yr), which is also consistent with slower uplift in times later than 1.5 Ma (Spotila et al., 2001). In contrast, the vertical fault model produces only ~0.4–0.7 mm/yr of relative uplift and cannot account for the geologic uplift rates. Vertical models with strike-slip rates as fast as 28 mm/yr though the restraining bend can produce 1–3 mm/yr of uplift adjacent to the fault (Smith and Sandwell, 2003); however such slip-rates greatly exceed the geologic observations within the restraining bend in the SGPR (Figure 5). Both of our models produce subsidence >1 mm/yr within the San Bernardino Basin, which is consistent with depositional rates of ~1 mm/yr in this valley (Matti and Morton, 1993).

Site Specific Geologic Slip Rates

We also compare the modeled slip rates at the Earth's surface with geologic rates obtained through specific paleoseismic and geomorphic studies (Figure 5). The modeled strike-slip rates along the San Bernardino strand of the SAF decrease to the southeast and correlate well with geologic slip rates. However, the vertical SAF model overestimates right-lateral slip rates at more sites along the San Bernardino strand of the SAF than the north-dipping model. Again, the north-dipping fault configuration shows a more favorable comparison to geologic observations than the vertical fault model. The strike slip rate data along the SJF cannot distinguish between the models due to the simplification of the modeled SJF.

The geologically observed, and model reproduced pattern of decreasing slip rate to the southeast along the San Bernardino strand of the SAF, demonstrates the significant spatial variability of slip rates along fault segments due to interaction with nearby faults. The discrepancy of some geologic slip rates on the San Bernardino fault segment with slip rates from geodetic block models (Meade and Hager, 2005) may reflect the inability of the block models to incorporate the region's geologic complexity.

Slip Transfer: San Andreas Fault to San Jacinto Fault

Right-lateral slip along the SAF is lowest for both models along the SGT/Garnet Hill strand, which is the area of greatest geometric complexity. This decrease in strike-slip rate along the SAF occurs at the same distance from the Cajon Pass as the greatest strike-slip rates along the SJF (Figure 5). This suggests that, in the model, strike-slip is transferred from the SAF to the SJF even though the faults are not hard-linked (connected). Within the models, the inefficiency of the restraining bend impedes strike-slip along the SAF allowing the SJF to absorb the excess strike-

slip (Figure 5). Slip can transfer between two separated faults as the shear stresses are transmitted through the intervening material producing a soft-link (e.g., Crider and Pollard, 1998; Roberts and Michetti, 2004). When slip cannot be accommodated on a fault due to an inefficient geometry, some of that slip is taken up by other faults and the remainder becomes off fault deformation.

Geomorphology and Regional Transpression

Although deformation is driven by N52°W right-lateral displacements at the edges of the model, the lack of applied *regional* transpression does not hinder the development of localized uplift in the north-dipping model. The contrasting uplift produced by the vertical and north-dipping SAF models indicates that dipping fault geometry can account for significant uplift without regional transpression. The inference that local fault configuration contributes to SBMuplift is consistent with the conclusions of several uplift studies in the region (e.g., Dibblee, 1975; Matti and Morton 1993; Spotila and Sieh, 2000; Spotila et al., 2007).

Preferred Fault Configuration

The vertical SAF model fails to match the geologic uplift pattern, overestimates slip rates at several sites along the San Bernardino strand of the SAF, and neglects the geologic and seismic indications of active north-dipping faults in the SGPR. Of the two models, we favor the north-dipping geometry for the San Andreas Fault through the SGPR.

Our results suggest that crustal deformation models for restraining bends that use only vertical faults will overestimate slip rates and underestimate off-fault deformation. The complexity of active faults through the SGPR may influence earthquake rupture scenarios because regions of fault surface complexity may be regions where ruptures initiate, terminate, or jump to other faults (e.g., Harris et al., 1991; Wald and Heaton, 1994). Earthquake rupture along the southern SAF may produce significant ground shaking within the metropolitan Los Angeles region (Olsen et al., 2006). Consequently, the constraints on fault geometry suggested here will help future rupture models of the southern SAF more accurately predict seismic hazards.

Conclusions of numerical models

Our, three-dimensional models confirm the geologic and geophysical evidence for north-dipping active fault segments along the SAF within the SGPR and demonstrate that non-vertical strike-slip segments can play a significant role in active deformation of restraining bends. Furthermore, incorporating geologic complexities, such as dipping fault surfaces, into numerical fault models, which is now more feasible than ever, increases the match between modeled results and geologic observations. For example, the uplift of the SMBs is better matched by active north-dipping faults within the restraining bend than by a vertical SAF. Similarly, the north-dipping SAF model better matches variable strike-slip rates at sites along the San Bernardino strand of the SAF. The match of the model results to the geologic observation of decreasing strike-slip along the San Bernardino strand of the SAF highlights the value of geologic timescale models that do not prescribe fault slip rates a priori. Within the models of the SGPR, the SJF picks up some of the strike slip that is lost to the SAF in an effort to by-pass the inefficient SAF geometry. This transfer occurs between soft-linked faults that have no physical connection. This study also reveals the sensitivity of uplift patterns and fault slip rates to fault geometry within

restraining bends. Our results highlight the need for crustal deformation models of restraining bends to carefully consider non-vertical strike-slip fault geometry.

Analog modeling setup

Analog models were set up using a soft clay material to simulate deformation of the crust across the plate margin at the San Bernardino Mountains. The computer-controlled rig is comprised of two plates, one stationary and the other driven by two orthogonal step motors (Fig. 6). For our configuration, the moving plate underlies crust to the east of the San Andreas fault and the stationary plate underlies material west of the San Jacinto fault. The region between the two faults is underlain by a plate that is attached to the moving plate by a lever arm. The length of this lever controls the partitioning of strain between the San Andreas and San Jacinto faults. For our models, the 45 mm/yr accommodated across these faults is partitioned as 10 mm/yr on the San Jacinto and 35 mm/yr on the San Andreas. Along the San Andreas north of the San Bernardino Mountains the equivalent of 45 mm/yr is applied. Actual strain rates on the system are ~1 cm/hour and the clay consists of well-mixed kaolinite and water. The clay pack is 3 cm thick, which scales to several kilometers of upper crust material.

At the start of the experiment, the faults are cut into the clay with a needle. The needle is dragged along wooden templates that ensure that correct trace and dip of each fault segment. For the results presented here, we simulate the configuration of the San Andreas with a north-dipping segment south of the San Bernardino Mountains (ie. the better fitting numerical model). We run a current through the needle to reduce the drag encountered by the needle pulled through clay. The electric current affects the charged clay bonds to effectively reduce the cohesion as the needle travels through the clay.

Analog modeling results and conclusions

The slip along the San Andreas in the analog model can be compared to the slip distribution in the numerical model and the slip rates inferred from geologic relationships (Fig. 7). Within the analog model the strike-slip rates decrease from the Cajon Pass to the San Gorgonio thrust region and then increase to the south along the Coachella segment of the San Andreas fault. Strike slip rates are negligible along the San Gorgonio thrust. The overall trend of the slip distribution matches that of the numerical results and the geologic data. Although deformation in both the numerical model and the analog model are driven by the same plate velocities, the lesser slip in the analog model indicates greater off fault deformation. The clay material can accumulate significant (>20%) contraction without fault slip. Such large deformation may over-estimate off-fault deformation in the region.

The uplift of the surface of the analog model can be compared with vertical surface displacements predicted by the numerical model (Fig. 8). For the analog experiment, uplift is measured with detailed laser scans of the clay surface. The laser scans produce digital elevation data that can be used to visualize uplift. Within both models the region representing the San Bernardino Mountains is uplifted and the region representing the San Bernardino basin is down dropped.

The close match of strike-slip distribution and pattern of off-fault deformation in both the analog and numerical models shows that analog models can be used to simulate first-order deformation in southern California.

REFERENCES CITED

- Allen, C.R., 1957, San Andreas fault zone in the San Gorgonio Pass, southern California: Geological Society of America Bulletin, v. 68, p. 315–350, doi: 10.1130/0016–7606.
- Anderson, R.S., 1990, Evolution of the northern Santa Cruz Mountains by advection of crust past a San Andreas fault bend: Science, v. 249, 4967, p. 397–401.
- Behr, W., Hudnut, K., Platt, J., Kendrick, K., Sharp, W., Fletcher K., Finkel, R., and Rood, D., 2007, A revised slip rate estimate for the Mission Creek–Coachella Valley strand of the southern San Andreas fault at Biskra Palms Oasis, Indio, California: Southern California Earthquake Center Annual Meeting, Proceedings with Abstracts, v. 17.
- Bennett, R.A., Davis, J.L., and Wernicke, B.P., 1999, Present-day pattern of Cordilleran deformation in the western United States: Geology, v. 27, p. 371–374, doi: 10.1130/0091–7613.
- Carena, S., Suppe, J., and Kao, H., 2004, Lack of continuity of the San Andreas fault in southern California: Three-dimensional fault models and earthquake scenarios: Journal of Geophysical Research, v. 109, B04313, doi: 10.1029/ 2003JB002643.
- Crider, J.G., and Pollard, D.D., 1998, Fault linkage: Three-dimensional mechanical interaction between echelon normal faults: Journal of Geophysical Research, v. 103, no. B10, p. 24,373– 24,391, doi: 10.1029/98JB01353.
- Dibblee, T., 1975, Late Quaternary uplift of the San Bernardino Mountains of the San Andreas and related faults: California Division of Mines and Geology Special Report 118, p. 127–137.
- Harris, R.A., Archuleta, R.J., and Day, S.M., 1991, Fault steps and dynamic rupture process: 2-D numerical simulations of a spontaneously propagating shear fracture: Geophysical Research Letters, v. 18, p. 893–896, doi: 10.1029/ 91GL01061.
- Kendrick, K.J., Morton, D.M., Wells, S.G., and Simpson, R.W., 2002, Spatial and temporal deformation along the northern San Jacinto fault, southern California; implications for slip rates: Seismological Society of America Bulletin, v. 92, p. 2782–2802.
- Langenheim, V.E., Jachens, R.C., Matti, J.C., Hauksson, E., Morton, D.M., and Christensen, A., 2005, Geophysical evidence for wedging in the San Gorgonio Pass structural knot, southern San Andreas fault zone, southern California: Geological Society of America Bulletin, v. 117, p. 1554–1572, doi: 10.1130/B25760.1.
- Matti, J.C., and Morton, D.M., 1993, Paleographic evolution of the San Andreas fault in southern California: A reconstruction based on new cross-fault correlation, *in* Powell, R.E., et al., eds., The San Andreas fault system: Displacement, palinspastic reconstruction, and geologic evolution: Geological Society of America Memoir 178, p. 107–159.
- Matti, J.C., Morton, D.M., and Cox, B.F., 1985, Distribution and geologic relations of fault systems in the vicinity of the central Transverse Ranges, southern California: U.S. Geological Survey Open-File Report 85–365, 23 p.
- Matti, J.C., Morton, D.M., and Cox, B.F., 1992, The San Andreas fault system in the vicinity of the central Transverse Ranges province, southern California: U.S. Geological Survey Open-File Report 92–354, 52 p.
- McGill, S., Weldon, R.J., II, Kendrick, K., and Owen, L., 2006, Late Pleistocene slip rate of the

- San Bernardino strand of the San Andreas fault in Highland: Possible confirmation of the low rate suggested by geodetic data: *Seismological Research Letters*, v. 77, no. 2, p. 279.
- McGill, S., Kendrick, K., Weldon, R.J., II, and Owen, L., 2007, Pleistocene and Holocene slip rate of the San Andreas fault at Badger Canyon, San Bernardino, California: Southern California Earthquake Center Annual Meeting, Proceedings with Abstracts, v. 17.
- Meade, B.J., and Hager, B.H., 2005, Block models of crustal motion in southern California constrained by GPS measurements: *Journal of Geophysical Research*, v. 110, B03403, doi: 10.1029/2004JB003209.
- Nicholson, C., 1996, Seismic behavior of the Southern San Andreas fault zone in the Northern Coachella Valley, California: Comparison of the 1948 and 1986 earthquake sequences: *Seismological Society of America Bulletin*, v. 86, p. 1331–1349.
- Olsen, K.B., Day, S.M., Minster, J.B., Cui, Y., Chourasia, A., Faerman, M., Moore, R., Maechling, P., and Jordan, T., 2006, Strong shaking in Los Angeles expected from southern San Andreas earthquake: *Geophysical Research Letters*, v. 33, L07305, doi: 10.1029/2005GL025472.
- Orozco, A.A., 2004, Offset of a mid-Holocene alluvial fan near Banning, CA; constraints on the slip rate of the San Bernardino strand of the San Andreas fault [M.S. thesis]: University of California at Northridge, 56 p.
- Plesch, A., and 27 others, 2007, Community fault model (CFM) for southern California: *Seismological Society of America Bulletin*, v. 97, p. 1793–1802, doi: 10.1785/0120050211.
- Roberts, G.P., and Michetti, A.M., 2004, Spatial and temporal variations in growth rates along active normal fault systems: An example from the Lazio-Abruzzo Apennines, central Italy: *Journal of Structural Geology*, v. 26, p. 339–376, doi: 10.1016/S0191–8141(03)00103–2.
- Rockwell, T., Loughman, C., and Merifield, P., 1990, Late Quaternary rate of slip along the San Jacinto fault zone near Anza, southern California: *Journal of Geophysical Research*, v. 95, no. B6, p. 8593–8605, doi: 10.1029/JB095iB06p08593.
- Shen, Z.K., Agnew, D.C., King, R.W., Dong, D., Herring, T.A., Wang, M., Johnson, H., Anderson, G., Nikolaidis, R., van Domselaar, M., Hudnut, K.W., and Jackson, D.D., 2003, The SCEC crustal motion map, version 3.0: Los Angeles, California, Southern California Earthquake Center.
- Smith, B.R., and Sandwell, D.T., 2003, Coulomb stress accumulation along the San Andreas fault system: *Journal of Geophysical Research*, v. 108, no. B6, 2296, doi: 10.1029/2002JB002136.
- Smith, B.R., and Sandwell, D.T., 2006, A model of the earthquake cycle along the San Andreas fault system for the last 1000 years: *Journal of Geophysical Research*, v. 111, B01405, doi: 10.1029/2005JB003703.
- Spotila, J.A., and Sieh, K., 2000, Architecture of transpressional thrust faulting in the San Bernardino Mountains, southern California, from deformation of a deeply weathered surface: *Tectonics*, v. 19, p. 589–615, doi: 10.1029/1999TC001150.
- Spotila, J.A., Farley, K.A., Yule, J.D., and Reiners, P.W., 2001, Near-field transpressive deformation along the San Andreas fault zone in southern California, based on

- exhumation constrained by (U-Th)/He dating: *Journal of Geophysical Research*, v. 106, no. B12, p. 30,909–30,922, doi: 10.1029/2001JB000348.
- Spotila, J.A., Niemi, N., Brady, R., House, M., and Buscher, J., 2007, Long-term continental deformation associated with transpressive plate motion: The San Andreas fault: *Geology*, v. 35, p. 967–970, doi: 10.1130/G23816A.1.
- Wald, D.J., and Heaton, T.H., 1994, Spatial and temporal distribution of slip for the Landers, California, earthquake: *Seismological Society of America Bulletin*, v. 84, p. 668–691.
- Weldon, R.J., II, and Sieh, K., 1985, Holocene rate of slip and tentative recurrence interval for large earthquakes on the San Andreas fault, Cajon Pass, southern California: *Geological Society of America Bulletin*, v. 96, p. 793–812.
- Weldon, R., Fumal, T., and Biasi, G., 2004, Wrightwood and the earthquake cycle: What a long recurrence record tells up about how faults work: *GSA Today*, v. 14, no. 9, doi: 10.1130/1052-5173(2004)014.
- Weldon, R., Fumal, T., Biasi, G., and Sharer, K., 2005, Past and future earthquakes on the San Andreas fault: *Science*, v. 308, p. 966–967, doi: 10.1126/science.1111707.
- Yule, D., and Sieh, K., 2003, Complexities of the San Andreas fault near San Geronio pass: Implications for large earthquakes: *Journal of Geophysical Research*, v. 109, no. B11, 2548, doi: 10.1029/2001JB000451.
- Yule, J., Fumal, T., McGill, S., and Seitz, G., 2001, Active tectonics and paleoseismic record of the San Andreas fault, Wrightwood to Indio: Working toward a forecast of the next “Big Event”, in Dunne, G., and Cooper, J., eds., *Geologic excursions in the Californian deserts and adjacent Transverse Ranges: Los Angeles, California, Pacific Section, SEPM (Society for Sedimentary Geology)*, p. 91–126.

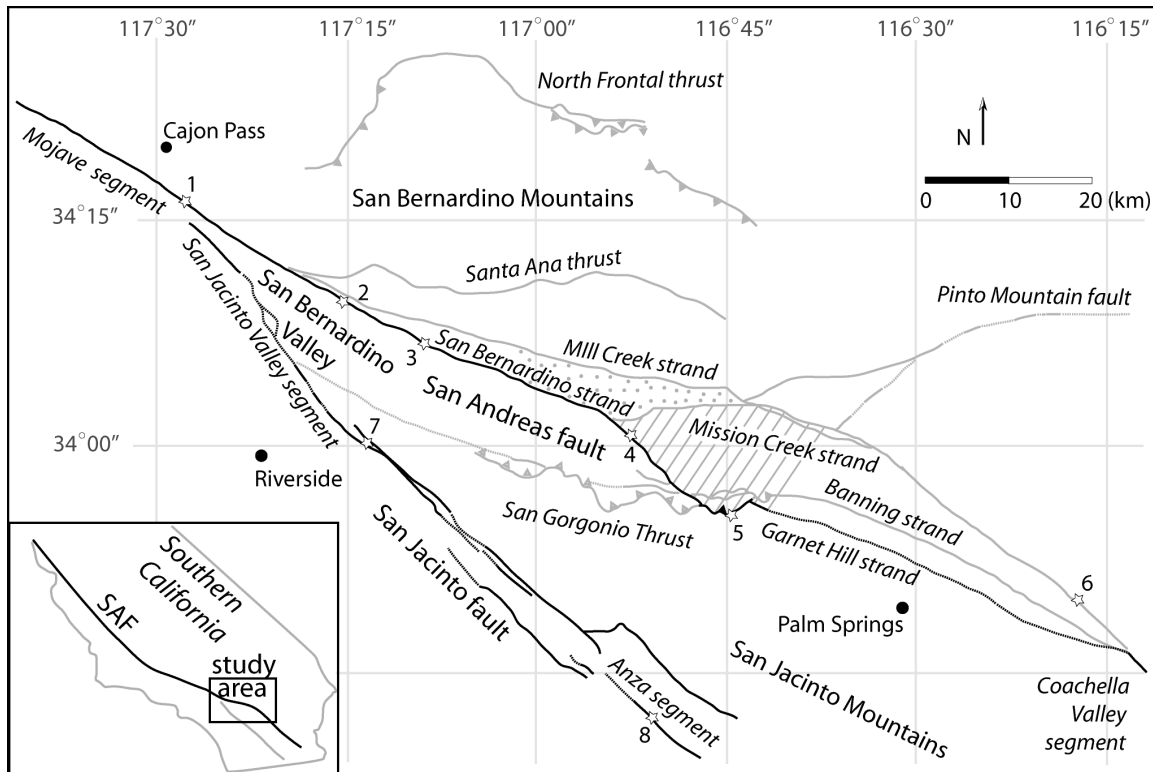


Figure 1. Fault trace map of the San Gorgonio Pass region. Model simulations of active faulting only include the black faults. The gray faults are secondary. Stars indicate locations of geologic study sites that have yielded slip rates. The dashed lines indicate faults that have no surface trace. The stippled section is the Yucaipa Ridge block while the cross-hatched section is the Morongo Block of the San Bernardino Mountains. Site 1, Cajon Pass– Weldon and Sieh, 1985; site 2, Badger Canyon– McGill, 2007; site 3, Plunge Creek- McGill et al., 2006; site 4, Burro Flats – Orozco, 2004; site 5, Yule et al., 2001; site 6 - Behr et al., 2007; site 7 - Kendrick et al., 2002; site 8 - Rockwell et al., 1990 and Rockwell, 2006 (modified from Matti et al., 1992).

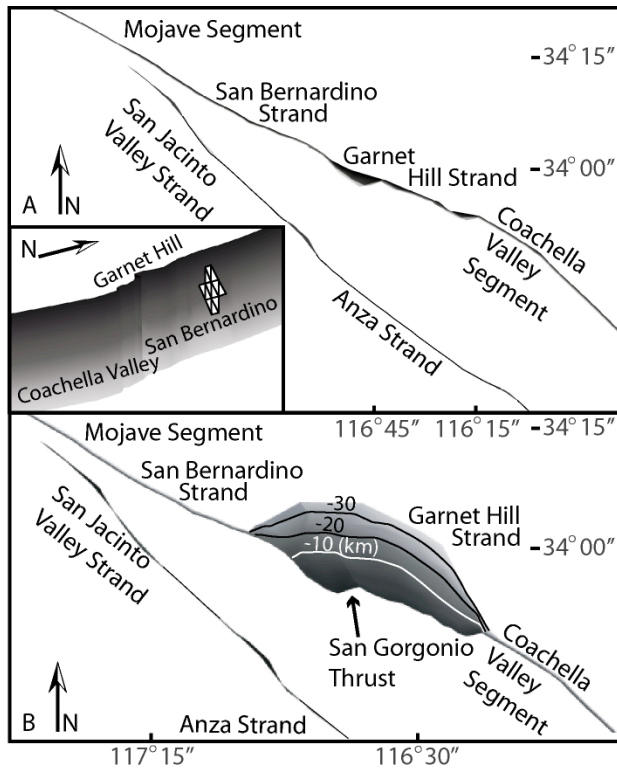


Figure 2. Schematic drawing of the loading of the models. The edges of the 35 km deep detachment as well as the distal tips of the primary faults have prescribed slip. The slip on the detachment is decreased incrementally as each section nears the strike-slip fault until slip on the section adjacent to the fault matches the prescribed slip on the fault tip. Away from the model boundaries all faults slip and interact in response to the loading at the edges.

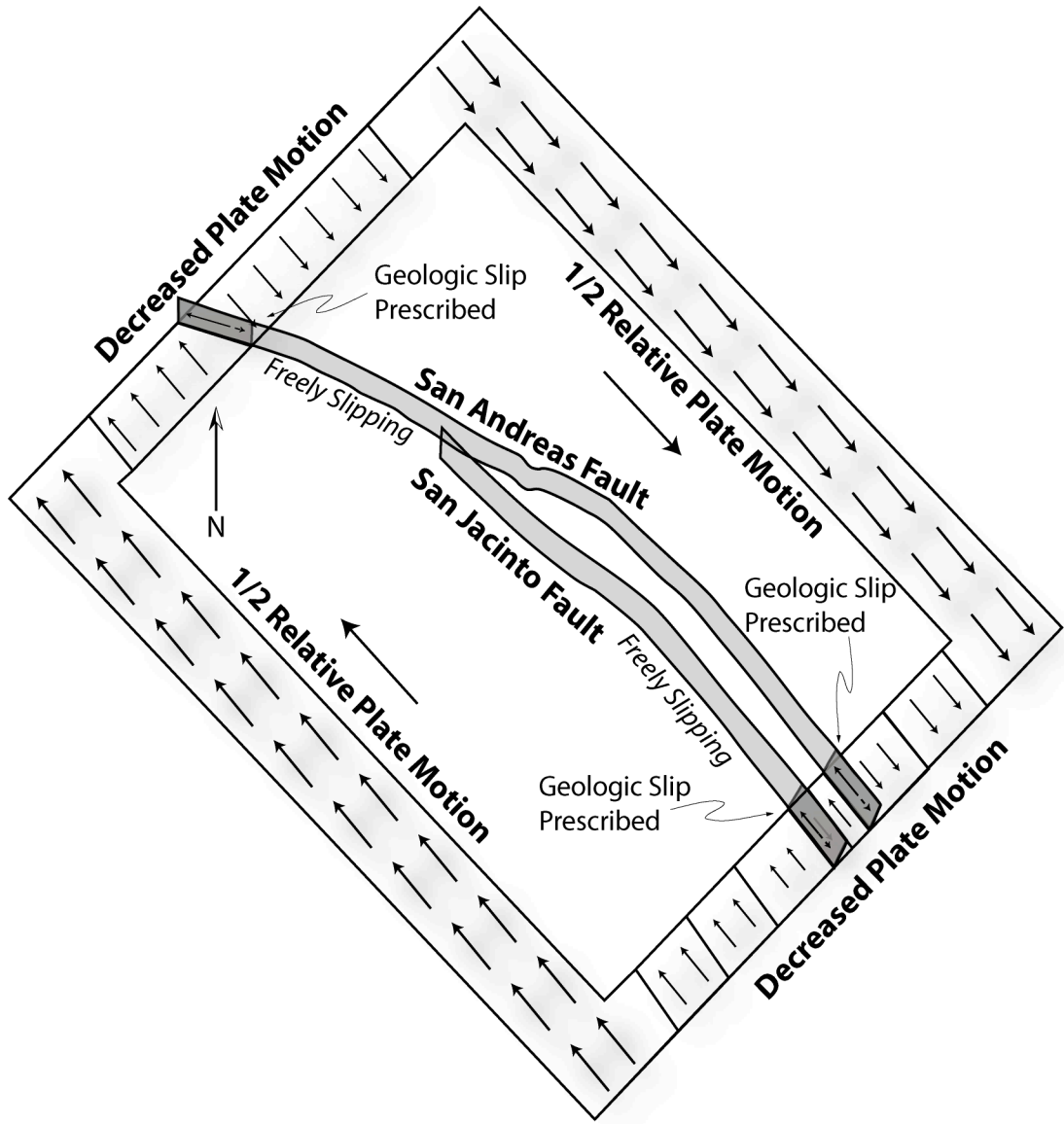


Figure 3. Map view of the A) vertical, B) north-dipping SAF geometries. Lighter shades indicate deepening depths to 35 km. Structure contours are overlain on dipping segments. The inset within A) shows a section of the mesh used for the fault surfaces.

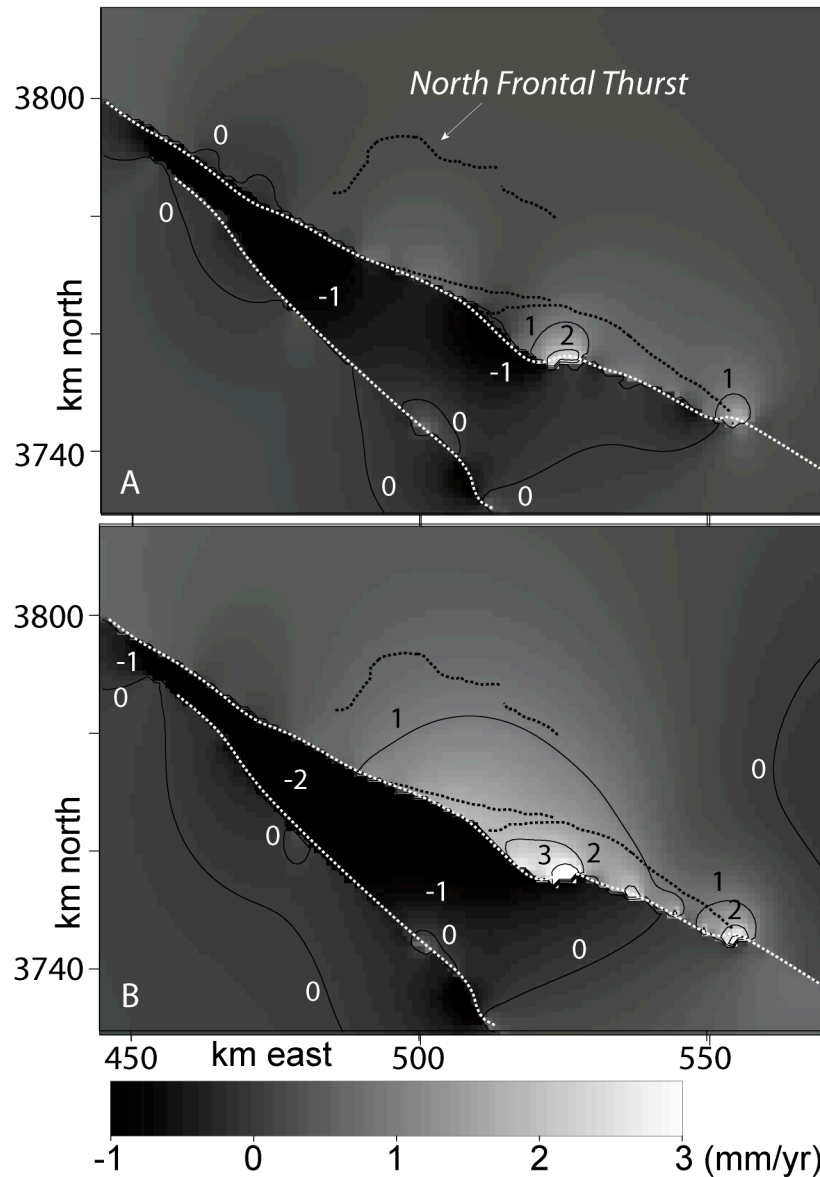


Figure 4. Vertical deformation maps for both models. Unlike the vertical model, the dipping models produce uplift within the region of the southern San Bernardino Mountains (e.g., the Yucaipa Ridge and Morongo Blocks (Figure 2.1). The dotted lines are faults (Figure 2.1).

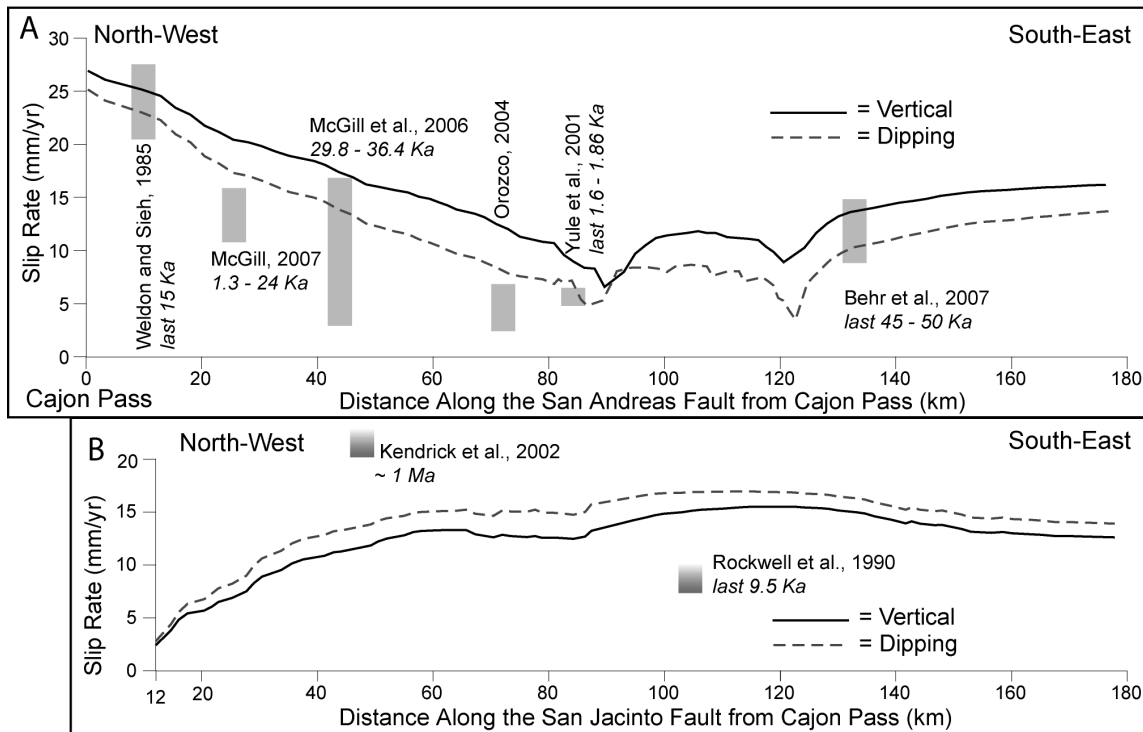


Figure 5. Surface strike-slip rates along the fault traces within the San Gorgonio Pass region. The graphs have been arranged so that the scales are the same and positioned according to distance from Cajon Pass. The northwestern half of plot A shows decreasing strike-slip rate along the San Bernardino strand of the San Andreas fault from Cajon Pass to the San Gorgonio thrust. The vertical, continuous model has the greater right-lateral slip rate along the San Andreas fault and exceeds geologic slip rates at more sites than the north-dipping model. The vertical San Andreas fault model has slower strike-slip rates than the north-dipping model along the San Jacinto fault in graph B. The gradational ranges indicate minimum slip rate estimates.

A



B



Figure 6: A) Analog model set-up. The right plate moves towards the camera while the left plate is stationary to simulate motions across the plate margin. Middle region moves towards the camera at a slower rate to capture the strain partitioning between the San Andreas and San Jacinto Faults. B) The clay cake at the start of the experiment. The faults are cut into the clay using a template as a guide.

San Andreas Fault

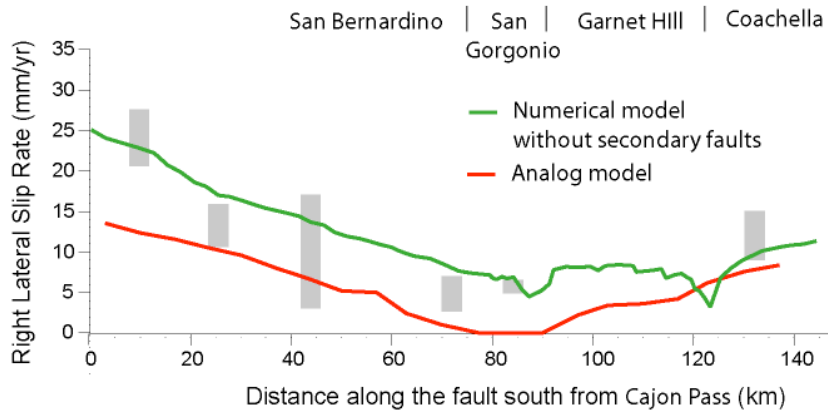


Figure 7: Slip distribution along the San Andreas fault for the analog (red) and numerical (green) models. paleoseismic rates are shown as grey bars (see Figure 5).

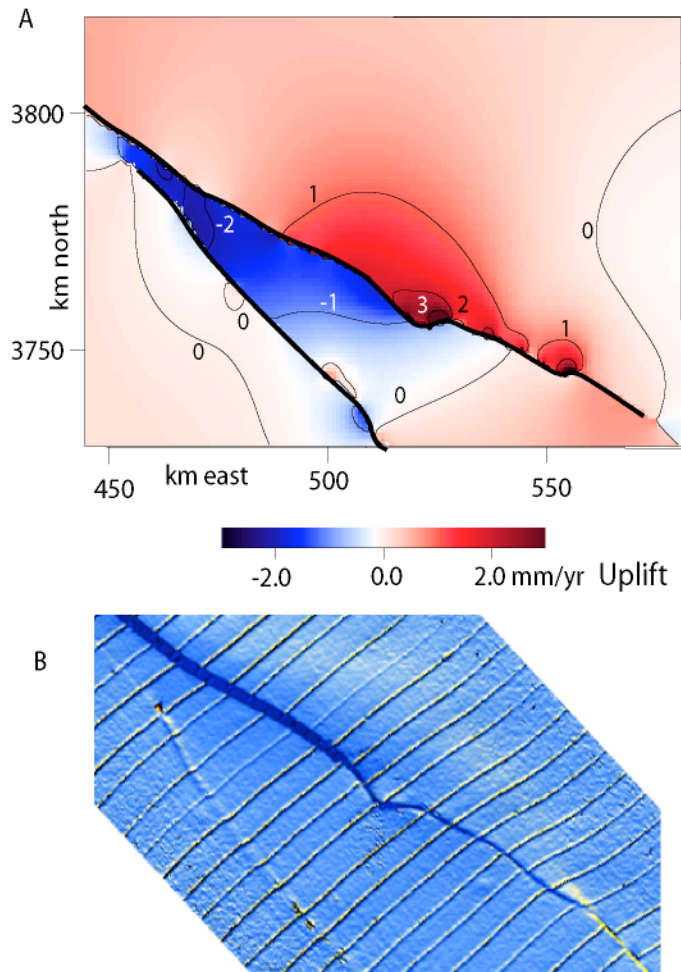


Figure 8. A) Uplift rates from the numerical model. B) Side lit image of the surface of the analog experiments at 250,000 years of deformation. The regions of uplift and subsidence within the analog model match the numerical model.

Bibliography of work related to this grant:

Dair, Laura and Michele L. Cooke, 2009. San Andreas Fault Topology Through the San Gorgonio Pass, California, *Geology*, v 37, p. 119-122; doi:10.1130/G25101A.1

Dair, Laura and Michele L. Cooke, in preparation. Recent Evolution of the San Andreas Fault at the San Gorgonio Knot, Southern California

Dair, Laura, Michele L. Cooke and Mario Del Castello, Numerical and Analog Models of the Evolution of the San Andreas Fault through the San Gorgonio Knot, *Geological Society of America Annual Meeting*

Cooke, Michele, Laura Dair and Mario Del Castello, Analog and Numerical Investigations into the Complexity of the San Andreas Fault through the San Gorgonio Knot, *Annual Meeting of the American Geophysical Union*